16th World Conference on Earthquake Engineering, 16WCEE 2017
Santiago Chile, January 9th to 13th 2017
Paper N° 3537
Registration Code: S-N1461601217

IDA & CLOUD METHOD FOR FRAGILITY ASSESSMENT OF BARE & INFILLED STEEL FRAME STRUCTURES

A. Nassirpour[(1)], B. Song[(2)], D. D'Ayala[(3)]

[(1)] *PhD Candidate, University College London – EPICentre, London-UK, a.nassirpour@ucl.ac.uk*
[(2)] *PhD Candidate, University College London – EPICentre, London-UK, biao.song.14@ucl.ac.uk*
[(3)] *Professor of Structural Eng., University College London – EPICentre, London-UK, d.dayala@ucl.ac.uk*

Abstract

In this study, the seismic performance of two- and four- storey steel framed structures has been assessed and compared in terms of capacity and fragility. Full scale three-dimensional models of the selected structures have been simulated once as bare steel frame and once while considering the effect of masonry infilled panels, to have the most realistic representation. Furthermore, the selected structures have been designed following two methods of only gravity loading and considering additional seismic excitation. The seismic behaviour has been evaluated through Incremental Dynamic Analysis (IDA) and the Cloud method (NLTHA). A comparison of resultant structural behaviour and fragility functions for both bare and infilled cases indicates that the structural effect of masonry infill panels should not be neglected, as they have a significant influence on the lateral stiffness, strength and ductility of the entire structural system and ignoring it would be hazardous.

Keywords: Incremental Dynamic Analysis (IDA); Cloud Method; Nonlinear Time History; Fragility Curve; Infilled Steel Frame

1. Introduction

An adequate approach to evaluate the performance of a structure under seismic excitation is through employing fragility curves. Many studies have investigated bare concrete and steel frame structures, while limited researches have been conducted on developing fragility curves for framed structures with masonry infilled walls.

Typically, steel framed structures, with unreinforced masonry infill panels, make up a considerable proportion of residential buildings in seismically active regions, such as Japan, China, Turkey, Iran and California. Moreover, in the past few decades, factors such as speedy execution, light weight and cost efficiency have made these structures more popular. The infill panels are widely used as external walls and interior partitions in buildings. When subjected to strong earthquake loads, these structures are at high risk of heavy damage, due to the complex composite interaction of the unreinforced masonry infills and their surrounding frames, which significantly effects the response of the structural system. These structures inherit a large amount of non-linear inelastic deformation, primarily because of material non-linearity. The infill panels stiffen and strengthen the building significantly at relatively early drift stages. Though, after passing the ultimate strength, a rapid strength drop can be observed due to failure of the panels. This sudden decrease in capacity is in contrary to the observed behaviour of bare steel frames and can become problematic [1]. However, in the prevailing structural analysis and design stages, the contribution of masonry infills is ignored and their presence is solely considered as non-structural permanent loading and a source of significant over-strength. Given the rising number of masonry infilled steel framed structures and limited information on seismic performance of such structures, fragility functions are urgently required.

Various methods have been proposed for evaluating the seismic performance and deriving fragility curves, each with its own pros and cons. Hence, the complexity, time requirement, and accuracy can vary significantly depending on the chosen method.

Performance-based earthquake engineering (PBEE) is the current trend in designing earthquake-resistant structures. The implementation of the PBEE framework requires the assessment of the structural capacity in

multiple earthquake hazard levels. The method requires accurate estimations of the seismic demand and capacity of structures. Cloud method and Incremental dynamic analysis (IDA) [2] are widely used parametric methods for assessing structural performance against earthquake loading. These methods enable direct evaluation of the record-to-record variability in structural response through a set of ground-motion records. If the number of ground-motion records is large enough, it can improve the accuracy significantly, however, the method becomes computationally demanding. Hence, in this study, following IDA and Cloud method, analytical fragility curves have been derived for bare steel frames and Masonry Infilled Steel Frame (MISF) structures by considering variation in the intensity of earthquake records. The disparity observed among the analysis methods and the resultant fragility curves will be investigated. Furthermore, by comparing the seismic performance of bare and infilled frames, the influence of masonry panels on overall performance will be analysed.

Cloud and IDA analysis can utilise the outcome of nonlinear dynamic analyses to estimate the distribution of demand given the intensity measure (IM). In IDA a structural model is subjected to a number of ground-motion records, each scaled to multiple levels of specific intensities. This approach requires a large number of nonlinear time history analyses (NLTHA) and is computationally expensive [3-5]. On the contrary, Cloud analysis does not employ specific IM levels, but instead uses either scaled or typically unscaled sets of records for analysis, resulting in a characteristic cloud of points in an IM-response plot. The selected suite of earthquake records should be capable of representing a broad range of values of the chosen intensity measure as they are not scaled. As a result, the record-to-record random properties in ground motions can be considered thoroughly.

The following discusses the variation observed in seismic analysis of full scale three-dimensional models by means of IDA and Cloud, allows a thorough comparison of both methods, while highlighting their pros and cons. The non-linear methods have been conducted by applying suites of real earthquake records to a two- and a four- storey steel frame building. The recorded performance points have been treated as input to derive analytical fragility curves.

2. Design & Modelling of Index Buildings

For this study, two generic frames have been chosen by considering a large database of common steel structures mainly constructed in middle-east region. A four stories high, four bay (5.0m), five frame (4.5m), unsymmetrical structure, with a floor height of 3.5m, representing mid-height structures and a two stories high, symmetric structure, with three bays (5.0m) and frames (5.0m), characterising the low-rise buildings have been designed and modelled.

All buildings have been designed following guidelines and recommendations of European standards, using ETABS (v.15) software. In order to represent low- and high- code seismic responses, each model has been designed under two different loading conditions, namely Gravity Loading and Seismic Loading. For the gravity loading, a simple steel frame (SGF) was designed, while for the seismic loading case, a Moment Resisting Frame (MRF) was selected. The seismic loading was applied by employing a type 1 spectrum of Eurocode 8, for semi-compact soil ($360m/s < V_{s,30} < 800m/s$) condition and a peak ground acceleration of 0.35g.

In terms of material property, steel material with S235 mechanical properties (f_y=235 MPa, $E=2.1\times10^5$ MPa, γ=78 kN/m^3) and C25/30 concrete for slabs were adopted, which are commonly used. The slabs have been designed as composite metal decks, with a total depth of 150mm. Both structures do not have any staircase core or bracing to act as a centre of stiffness.

Each structure has been modelled in three dimensions using fibre based finite element software SeismoStruct [6]. The software is capable of predicting large displacement behaviour of space frames under static and dynamic loadings, taking into consideration the geometric nonlinearities (e.g. P-Δ and P-δ) and material inelasticity. The following briefly discusses the modelling concepts and structural characteristics of each model.

The behaviour of steel material was simulated after Menegotto-Pinto steel model, which follows a uniaxial bilinear stress-strain model with kinematic strain hardening. Furthermore, to observe the influence of masonry panels on strength, lateral stiffness and ductility of the whole structural system, two cases have been defined for each of the mentioned structural models. In one case, the frame has been designed and modelled following the traditional practice, thus the contribution of infill panels was solely considered as permanent load on designated

beams. This is how most designers and codes expect the building to behave. While, in the second case, the actual behaviour of the infill panels under seismic excitation has been simulated in the analysis process.

In the past recent years, the concept of simulating the infill with a single or multiple diagonal struts under compression is widely accepted as a simple and rational way to describe the influence of the masonry panels on the surrounding frames and has been adopted in many documents and new guidelines, such as S304.1 (CSA, 2004), SEI 41-06 (ASCE, 2006), NZSEE (2006), MSJC (2010). The infilled frame structures need a realistic model and cannot be modelled as elasto-plastic system due to the stiffness and strength degradation especially in short period structures in which the hysteresis loops and energy dissipation capacity have a strong influence on the response. Furthermore, the location and the dimensions of openings play an important role in the strength and lateral stiffness of single panels and the whole structural system.

To this extent, a numerical macro model proposed by Crisafulli [7] is adopted for simulating the solid infills and those with openings. Following the equivalent strut approach, Crisafulli adopted the double-strut model which is accurate enough to describe the local effects resulting from the interaction between infill panel and its surrounding frame. The model, is able to consider the lateral stiffness and the strength of the masonry, particularly when a shear failure along mortar joints or diagonal tension failure is expected. A drawback of the model is its lack of capability to predict properly the bending moment and shear forces in the surrounding frame, since the panel is connected to the beam-column joints of the frame. However, in this regards, limited cases of shear failure in the steel frame have been observed and in most cases the infill panel fails before the steel frame. Moreover, this analytical model is capable of simulating the most common types of masonry panel failures, known as shear failure and diagonal tension failure. It should be noticed that although the model is also capable of considering the out–of–plane failure of infill walls, it has been ignored in this study as it is unlikely due to the arching mechanism.

In order to increase modelling accuracy, the masonry infill models have to be calibrated with the identical material used in construction of the index buildings under study. For this reason, an experimental research conducted by Tasnimi & Mohebkhah [8] on the behaviour of brick-infilled steel frame with and without opening has been selected. The materials used for the pseudo-dynamic tests are of great similarly to those available and commonly used for in construction.

Representing the masonry material, nominal 219×110×66 mm solid clay bricks (with no voids) placed in running bond with Portland cement type 1 and sand mortar. The average prism compressive strength of the infill panel has been evaluated following ASTM C-1314 and C-10. A full solid infill panel (f_m=7.4 MPa) and one with large window opening (f_m=8.5 MPa) located at its centre (ratio=0.176) have been calibrated with the experimental results. For calibration was conducted on single-storey, single-bay steel frame specimens, tested under in-plane cyclic loading applied at the top corner of the frame (Fig. 1 and Fig. 2). The models are set to be as realistic as possible by considering the location of masonry infills, lateral stiffness, strength of the elements and the effect of any opening (door and windows) on the panels.

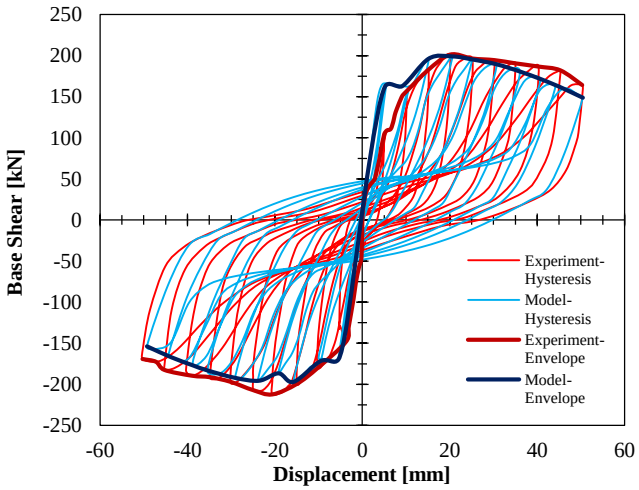

Fig. 1 - Backbone and hysteresis curve showing calibration of solid infill

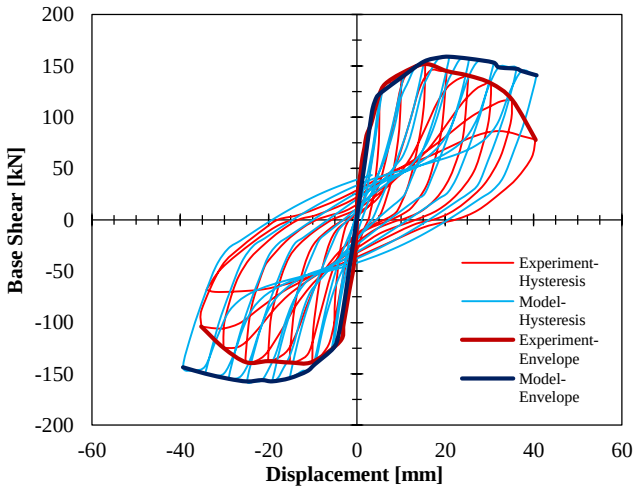

Fig. 2 - Backbone and hysteresis curve showing calibration of infill with opening

Table 1 summarises the structural characteristics, including the fundamental period (T_1) and mass, of each analysed model.

Table 1 - Characteristics of the models

No.	Structural Description	HAZUS Category	T1 [s]	T2 [s]	Mode 1 [Hz]	Mode 2 [Hz]	Mass [tonnes]
1	2 Storey - SGF-Bare	S1L Low Code	0.68	0.62	1.47	1.61	103
2	2 Storey - SGF-Infill	S5L Low Code	0.27	0.22	4.00	4.76	103
3	2 Storey - MRF-Bare	S1L High Code	0.40	0.39	2.63	2.53	107
4	2 Storey - MRF-Infill	S5L High Code	0.24	0.20	4.63	5.38	107
5	4 Storey - SGF-Bare	S1M Low Code	1.85	1.79	0.54	0.56	1'082
6	4 Storey - SGF-Infill	S5M Low Code	0.72	0.66	1.39	1.52	1'082
7	4 Storey - MRF-Bare	S1M High Code	1.45	1.39	0.69	0.72	1'091
8	4 Storey - MRF-Infill	S5M High Code	0.68	0.63	1.47	1.60	1'091

3. Ground Motion Selection

As the results of nonlinear dynamic analysis are highly sensitive to the applied ground motion records, it is essential that the selected set reflects the seismic hazard of the particular site and that the scaling is legitimate [9]. If these two conditions are not satisfied, a bias in the structural response may occur, which can be reduced by careful selection of a suitable set of records [10-12]. Moreover, there are several issues of efficiency and sufficiency associated with the IM selection. Since there are no directivity-influenced records in the suite and all buildings are of low to medium height (i.e. first-mode-dominated), the spectral pseudo-acceleration corresponding to the first-mode elastic vibration period and 5% damping ratio is chosen.

An extensive study for evaluation of ground-motion selection and modification methods has been prepared by FEMA P695 [13], which is implemented for the IDA in this study. The ground motions include 22 record pairs, each with two horizontal components for a total of 44 ground motions. The records have a magnitude range from M_W 6.5 to M_W 7.6 with an average magnitude of M_W 7.0 and all were recorded at sites located greater than or equal to 10 km from the fault rupture. Following the Eurocode 8 Soil classification, 16 sites are classified as stiff soil site and the remaining classified as very stiff soil. In order to reduce the computational effort, only the component with highest peak ground acceleration has been employed, leading to 20 ground motions (Fig. 3). The shortlisted records were scaled to different spectral acceleration (S_a) levels, ranging from 0.05g to 2.6g, with 0.05g steps (a total of 52 analyses for each selected record). It is thus an unavoidable fact that the IDA curves display large record-to-record variability, while the record scaling gives the opportunity to cover the entire range of structural response, from elasticity, to yielding and finally collapse. The spectral shape of mentioned ground motions was not a criterion in the selection process, as the FEMA P695 far-field ground motion sets are independent of site hazard or structural type. Therefore, the applied records are not reliant on period, any building-specific property of the structure and hazard disaggregation.

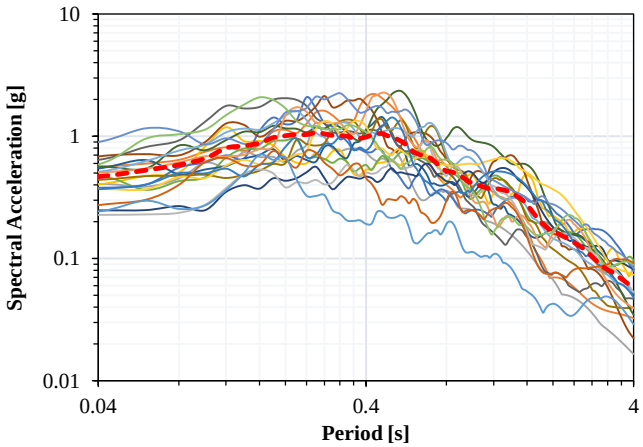

Fig. 3 - Response spectra of twenty individual components of the normalised far-field records of FEMA P695

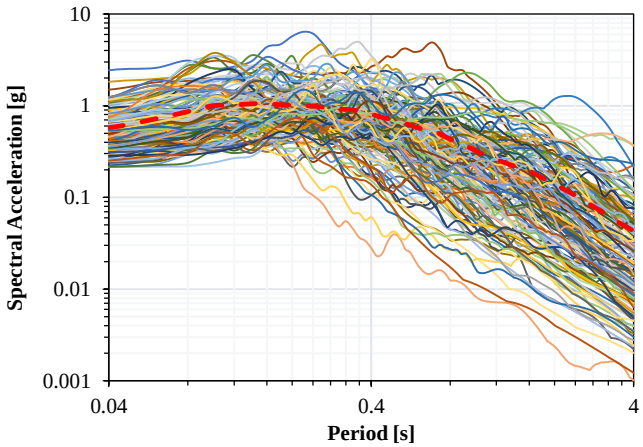

Fig. 4 - Response spectra of 150 individual components of SIMBAD

For cloud analysis, the 3rd version of SIMBAD database [14] has been chosen, consisting of 467 three-component accelerograms. Similar to IDA, from each accelerogram only the component with highest peak ground acceleration has been employed, leading to 150 ground motions (Fig. 4). The suite consists of worldwide shallow crustal earthquakes with moment magnitudes (M_W) ranging from 5.0 to 7.3 and epicentral distance (R_{epi}) approximately less than 30 km. This extensive range, ensures to provide records which can consider a vast design condition without introducing scaling factors. Furthermore, the high number of selected record give the opportunity of considering a vast variation of fundamental periods.

4. Nonlinear Dynamic Analysis

Nonlinear time history analysis (NLTHA) has been carried out on the models by implementing the unscaled earthquake records of SIMBAD database. Furthermore, a static pushover analysis was performed on each of the models and compared to NLTHA results (Fig. 5 and Fig. 6). Similar to the concept of the Intensity Measure (IM), which is introduced to better describe the scaling of a ground motion record, different engineering demand parameters (EDP) exist to measure the structural response and help quantify the damage. The demand parameter can be application-specific. For instance, the Maximum Peak Inter-Storey Drift Ratio (MIDR [%]) is known to relate well to global dynamic instability [15] and a decent EDP criteria for derivation of fragility functions.

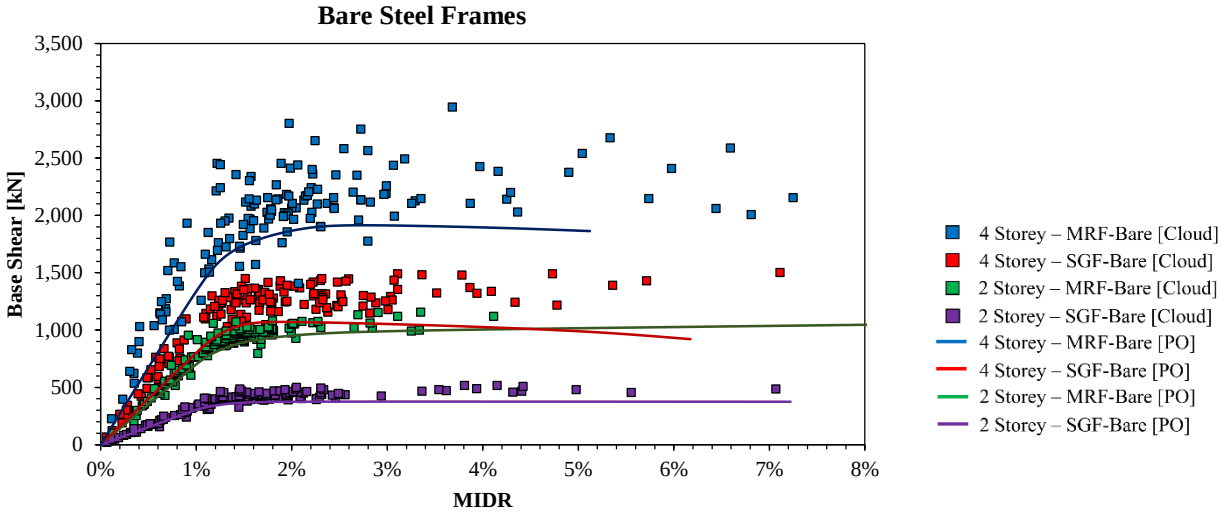

Fig. 5 – NLTHA and static pushover results for bare structures

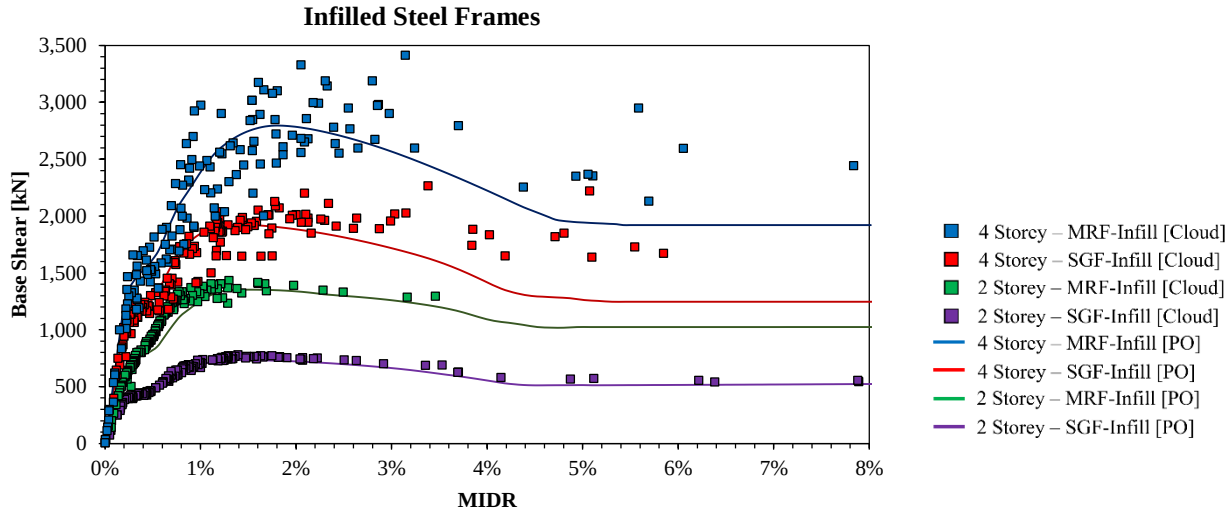

Fig. 6 – NLTHA and static pushover results for infilled structures

In the elastic region, the NLTHA points of all models were following the path of pushover curve. The dispersion starts in the inelastic region and mainly at higher capacities. For instance, in both cases of 4 storey MRF, either bare or infill, scattered data can be observed after passing the yield point. In general, the pushover curve is indicating a conservative behaviour of the structure.

Furthermore, it is clear that the seismic design (MRF) of structures has a significant effect on the overall capacity. The same is true when comparing bare and infilled frames, in which the presence of infill causes a considerable increase in the stiffness and strength of the structure. However, the issue arises after passing peak point, due to failure of most infill panels, a sudden drop, reduces the capacity substantially. This swift reduction of capacity can lead to soft storey failure, which is commonly observed in such structures.

The Incremental Dynamic Analysis has been conducted following the recommendation in ATC-63 [13] and ATC-58 [16]. The selected models were subjected to a suite of ground motion accelerograms, scaled to increasing levels of intensity measure (IM) until collapse is reached. The definition of collapse in this numerical study can be defined either as global dynamic or numerical instability occurring in analysis or an unusual large increase in storey drift associated with any small increment in spectral acceleration.

The Cloud (150 SIMBAD EQs) and IDA (1'040 analysis) results are presented in terms of Spectral Acceleration at the first-mode period of the structure ($S_a(T_1)$ [g]), representing the IM, versus Maximum Peak Inter-Storey Drift Ratio (MIDR [%]), demonstrating the structural demand (EDP). By estimating the representative percentile values given the range of $S_a(T_1)$ values, the outcomes have been further summarized into the 16th, 50th (median) and 84th fractiles of IDA curves (Fig. 7 and Fig. 8).

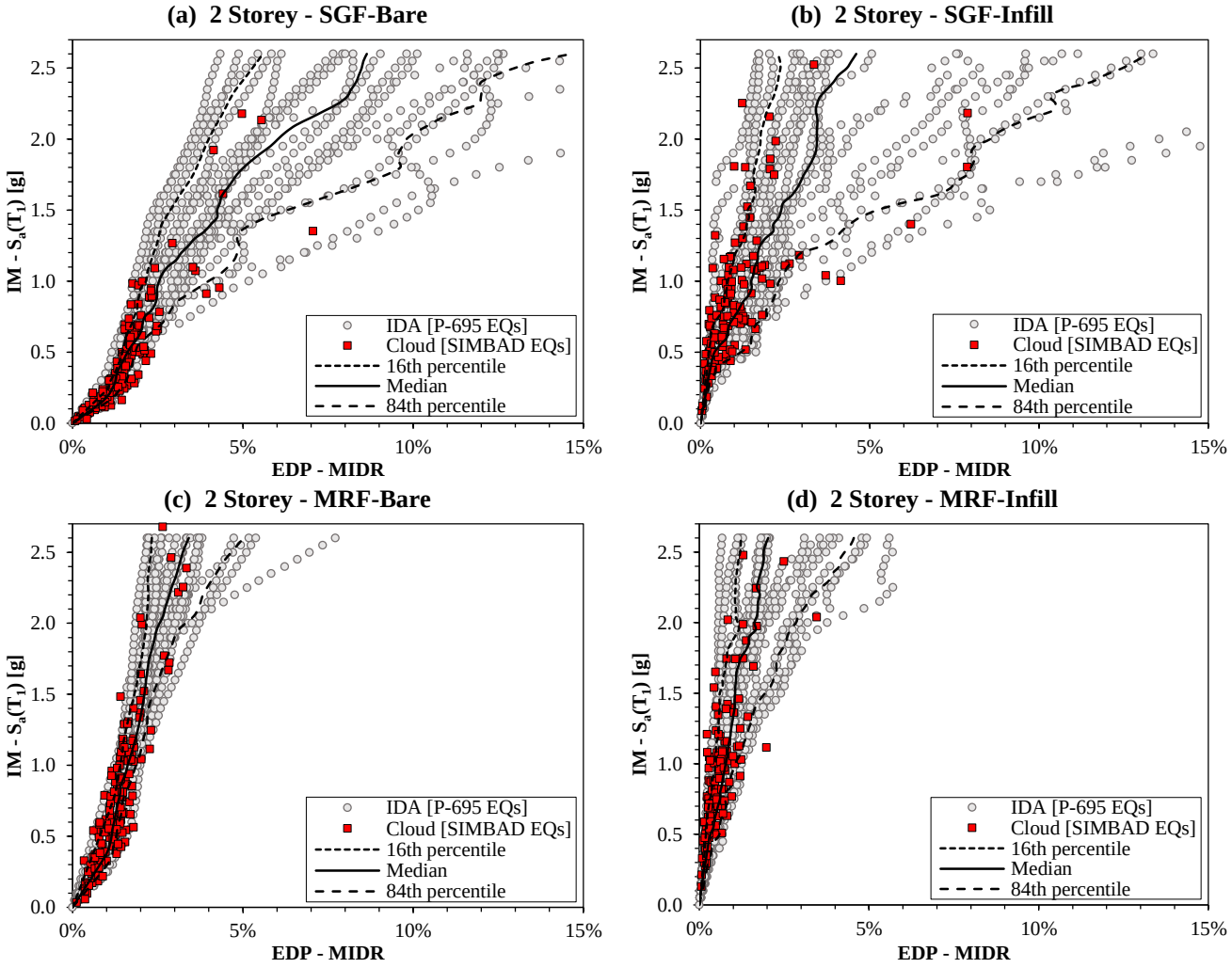

Fig. 7 – IDA and Cloud results for 2 storey structure

Since, IM and EDP have a direct correlation in the elastic region, both IDA and Cloud performance points, initiate as straight lines with minor dispersion at lower values of inter-story. In case of cloud data, at higher IM values, due to lack of stronger records, only a few performance points are present. Due to the nature of the applied record and capacity of the building, the structure may fail at lower IM values and the model is not capable of fulfilling the entire range (i.e. up to 2.6g). For instance, this condition is more evident for 4 Storey Bare Frame (SGF and MRF), in which after a certain intensity, the collapse stage is reached for most of the applied earthquakes and therefore no data on structural drift is recorded.

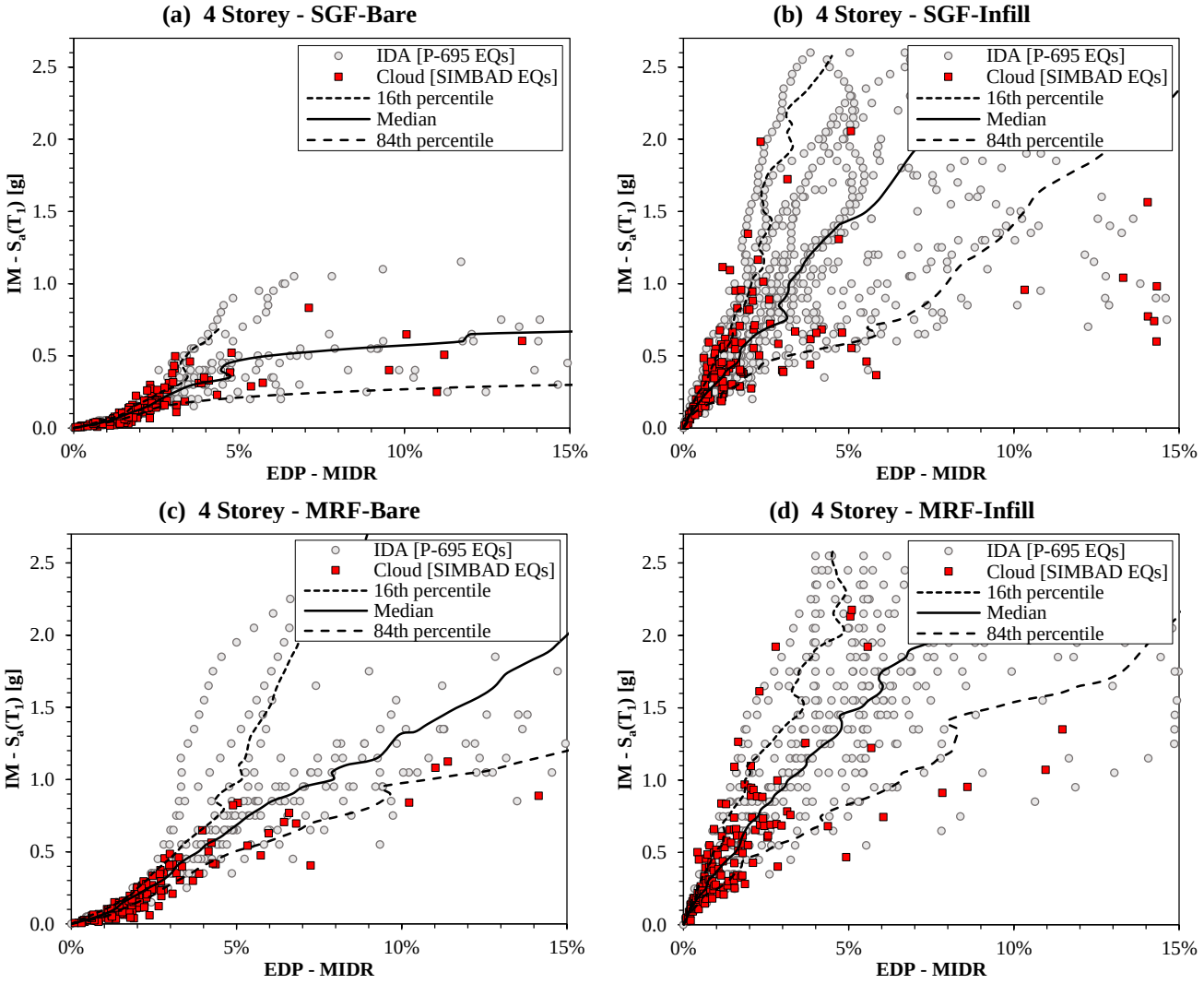

Fig. 8 - IDA and Cloud results for 4 storey structure

5. Defining Damage Limit States

In order to develop realistic fragility curves, it is necessary to assign rational "Damage States" for each of the structural elements. Hence, considering the damage states suggested in HAZUS-MH MR5 [17] and FEMA 356 [18] a number of criteria have been defined for three conditions. Moreover, as the infilled models have a composite structural system, where the initial lateral resistance is provided by the masonry infill walls, the damage thresholds have been specified based on the experimental damage observed in Tasnimi & Mohebkhah (2011) study. Accordingly, three of slight, moderate and extensive have been defined for the overall damage of the building based on the performance level of the structure subjected to a given earthquake intensity as follows:

1) *Slight:* hairline cracks (diagonal or horizontal) appear on some of the infill walls, some bricks near the beam-column interaction start to break and crush. Some steel members reach their yield point.

2) *Moderate:* large cracks (diagonal or horizontal) on most infill walls, a number of bricks dislodged and fall, partial and full collapse of few walls, some walls may bulge out-of-plane, failure at some steel connections, as some critical members may fail, and the structure might undergo a permanent lateral deformation.
3) *Extensive:* total failure of many infill walls and loss of stability of steel frame, bracings and moment connections start to fail, some infill walls may bulge out-of-plane, consequently the structure loses its lateral resistance. Some steel frame connections may have failed. Structure may exhibit permanent lateral deformation or partial collapse due to failure of some critical members.

In order to refer the mentioned damage states to the global structural behaviour, the damage thresholds have been defined in terms of MIDR. The damage index values used for the fragility analysis are given in Table 2. Any exceedance of the selected damage index from the corresponding value associated with each of these performance levels means fragility of the system is in that specific performance level. It is evident, that the threshold values vary depending on the characteristics of each structure. For comparison, the values suggested by HAZUS-MH MR5 are also presented.

Table 2 – Maximum peak inter-story drift ratio values assigned to different damage states for each model

Structural Description	HAZUS Classification	HAZUS Values			Applied Values		
		Slight	*Moderate*	*Extensive*	*Slight*	*Moderate*	*Extensive*
2 Storey-SGF-Bare	S1L Low Code	0.60%	1.00%	2.00%	0.93%	2.02%	3.52%
4 Storey–SGF-Bare	S1M Low Code	0.40%	0.64%	1.35%	0.69%	1.48%	2.28%
2 Storey–MRF-Bare	S1L High Code	0.60%	1.20%	3.00%	0.92%	2.33%	4.03%
4 Storey–MRF-Bare	S1M High Code	0.40%	0.80%	2.00%	0.88%	1.99%	2.98%
2 Storey–SGF-Infill	S5L Low Code	0.30%	0.60%	1.50%	0.41%	1.33%	3.48%
4 Storey–SGF-Infill	S5M Low Code	0.20%	0.40%	1.00%	0.38%	1.65%	3.47%
2 Storey–MRF-Infill	S5L High Code	-	-	-	0.54%	1.54%	3.45%
4 Storey–MRF-Infill	S5M High Code	-	-	-	0.48%	2.00%	4.04%

The observed difference between HAZUS thresholds and the ones applied, can be explained by looking at the idealised capacity curve suggested in HAZUS (Fig. 9). In case of bare steel frame, although the initial stiffness is in good agreement, the yield and ultimate strengths differ significantly. The same applies for the low code infilled structures and also, the capacity reduction after reaching peak strength is ignored by HAZUS. It should be noted that HAZUS does not propose any damage threshold, nor capacity curve, for high code (MRF) structures.

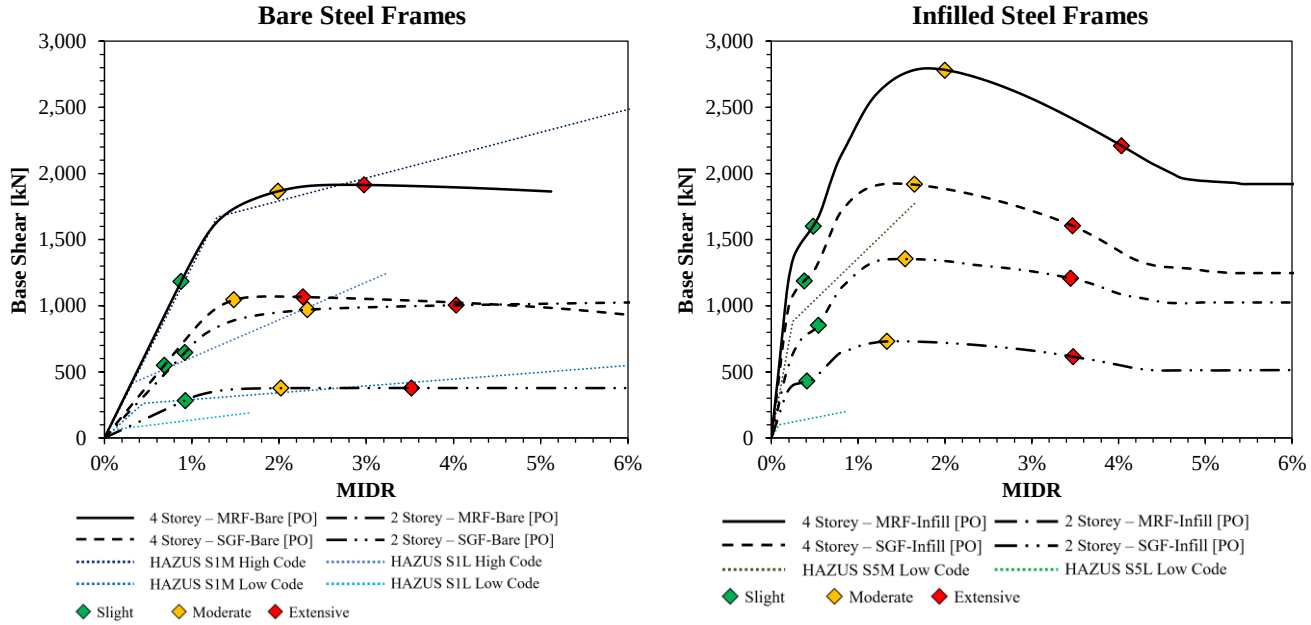

Fig. 9 – Damage thresholds defined for each structure

6. Fragility Derivation

The analytical fragility functions of each structure under study are derived by fitting a parametric model to the performance points obtained from IDA and Cloud analysis. Since there are no directivity-influenced records in the earthquake suite and all selected buildings are of low to mid height (i.e. first-mode-dominated), to characterise the intensity of earthquakes (IM), the spectral pseudo-acceleration corresponding to the first-mode elastic vibration period ($S_a(T_1)$) and 5% damping ratio is chosen. Furthermore, as previously mentioned, maximum peak inter-story drift ratio (MIDR) has been adopted as the engineering demand parameter (EDP).

To observe the variance caused by using different fitting techniques, three common ones have been compared. Maximum Likelihood [19], Least Square method [20] and Generalised Linear Regression method (GLM) with complementary log-log link function [21] have been applied. An example of fragility curves obtained, for 2 storey - SGF-Infill, using each of the mentioned methods is shown in Fig. 10. A thorough discussion on the mentioned statistical procedures for developing fragility function fitting can be found in Lallemant et al. [22] and Baker [20]. Comparing the resultant fragility functions indicates that due to high number of performance points, all three fitting methods result in similar curves, with very minor disparity and all are enclosed by the confidence intervals. However, due to smaller number of performance points passing the moderate and extensive limit state, the confidence bound for cloud analysis are considerably wider compared to the ones of IDA.

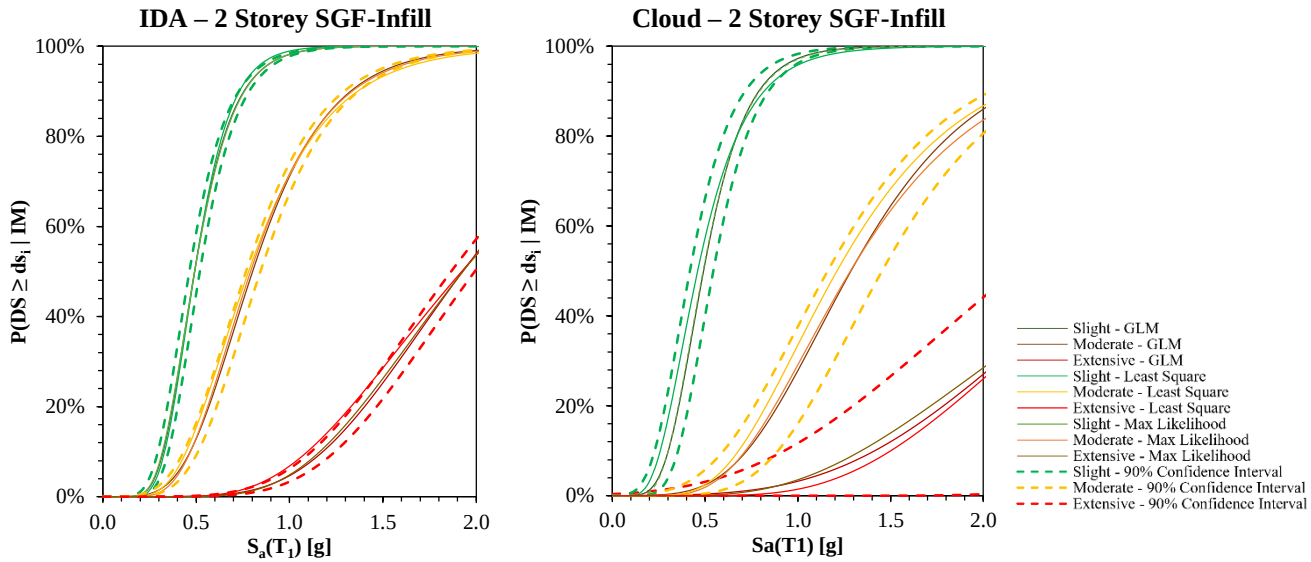

Fig. 10 - Comparing different fragility fitting functions for IDA and Cloud results of 2 storey – SGF-Infill

Achieving comparable fragility curves by different methods, the least square regression is used for all fragility derivations. In least square regression, the Median (μ) and Dispersion (β) (i.e. standard deviation of *ln(IM)*) parameters are estimated in a way to minimise the sum of squared errors (SSE) between the probabilities predicted by the fragility function and the fractions observed from the data (Eq. 1).

$$\mu, \beta = argmin_{\mu,\beta} \sum_{i=1}^{m} \left(\left(\frac{z_i}{n_i} \right) - \Phi \left(\frac{\ln(x_i / \mu}{\beta} \right) \right)^2 \quad (1)$$

where, m is the number of IM levels, z_i/n_i is the observed ratio of any building passing a certain damage state at IM=x_i , $\Phi(\,)$ is the standard normal cumulative distribution function (CDF).

The fragility curves derived for each of the Cloud and IDA methods are presented in Fig. 11 and Fig. 12, followed by their median and dispersion values. Generally, the median values of both Cloud and IDA are acceptably close. While, the dispersion values, due to the nature of each method, differs greatly. As expected, both methods have adequate fragility curves for lower damage states, mainly due to concentration of performance points of Cloud method at lower intensity measures. However, as the number of performance point for higher intensities drops and their dispersion rises, the resultant fragility curves are less representative of the structure's actual behaviour.

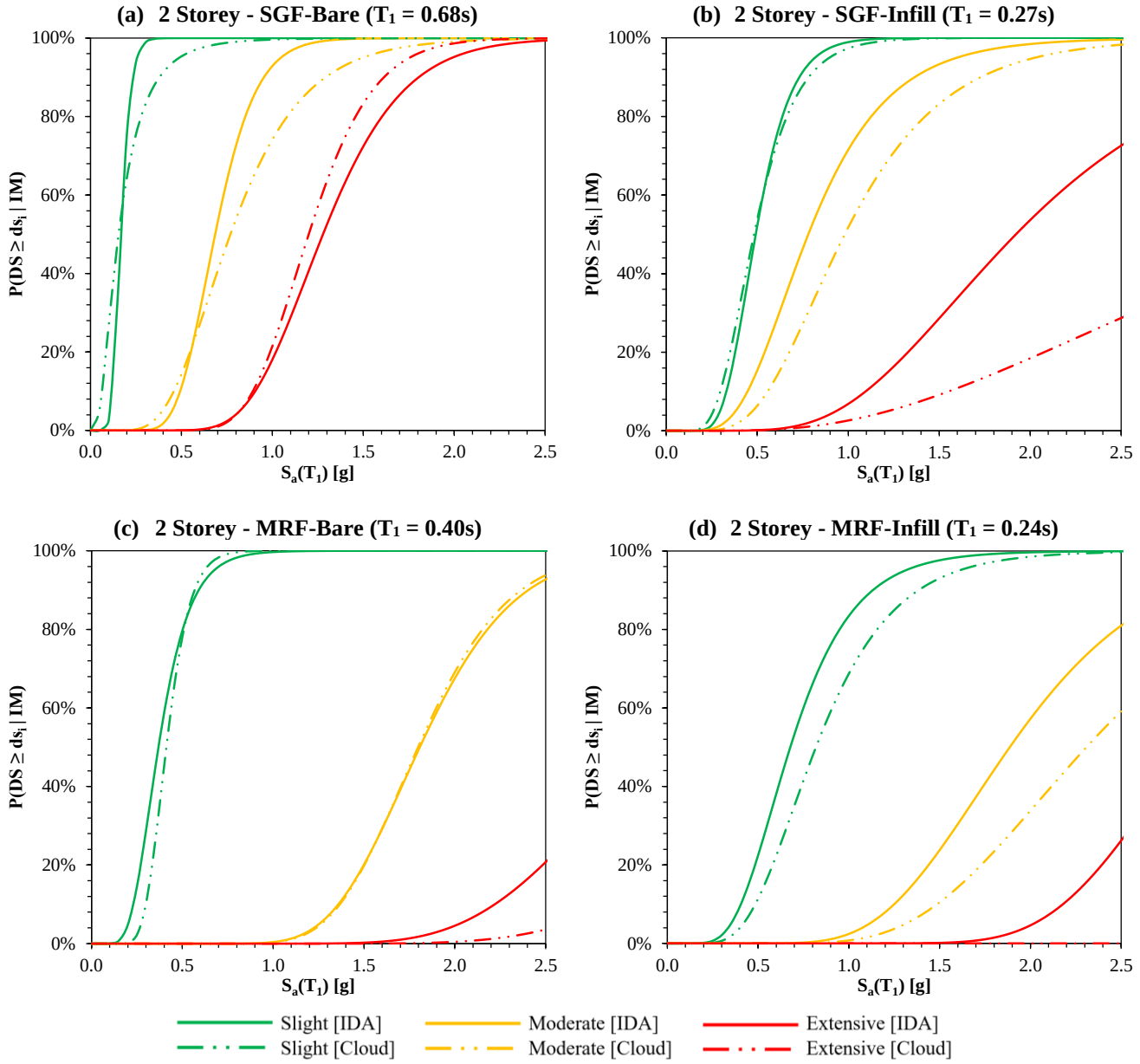

Fig. 11 – Fragility curves derived for 2 storey structures with different characteristics

Table 3 - IDA Fragility Functions - Median (μ [g]) and Dispersion (β) values for 2 storey structure

2 Storey IDA	SGF-Bare		SGR-Infill		MRF-Bare		MRF-Infill	
	μ	β	μ	β	μ	β	μ	β
Slight	0.17	0.26	0.49	0.31	0.37	0.37	0.21	0.27
Moderate	0.69	0.26	0.78	0.44	1.81	0.22	0.57	0.36
Extreme	1.28	0.27	1.92	0.44	3.08	0.26	1.16	0.46

Table 4 - Cloud Fragility Functions - Median (μ [g]) and Dispersion (β) values for 2 storey structure

2 Storey Cloud	SGF-Bare		SGR-Infill		MRF-Bare		MRF-Infill	
	μ	β	μ	β	μ	β	μ	β
Slight	0.15	0.70	0.48	0.38	0.41	0.25	0.82	0.41
Moderate	0.93	0.33	0.98	0.44	1.80	0.21	2.31	0.34
Extreme	1.20	0.23	3.63	0.66	4.12	0.28	-	-

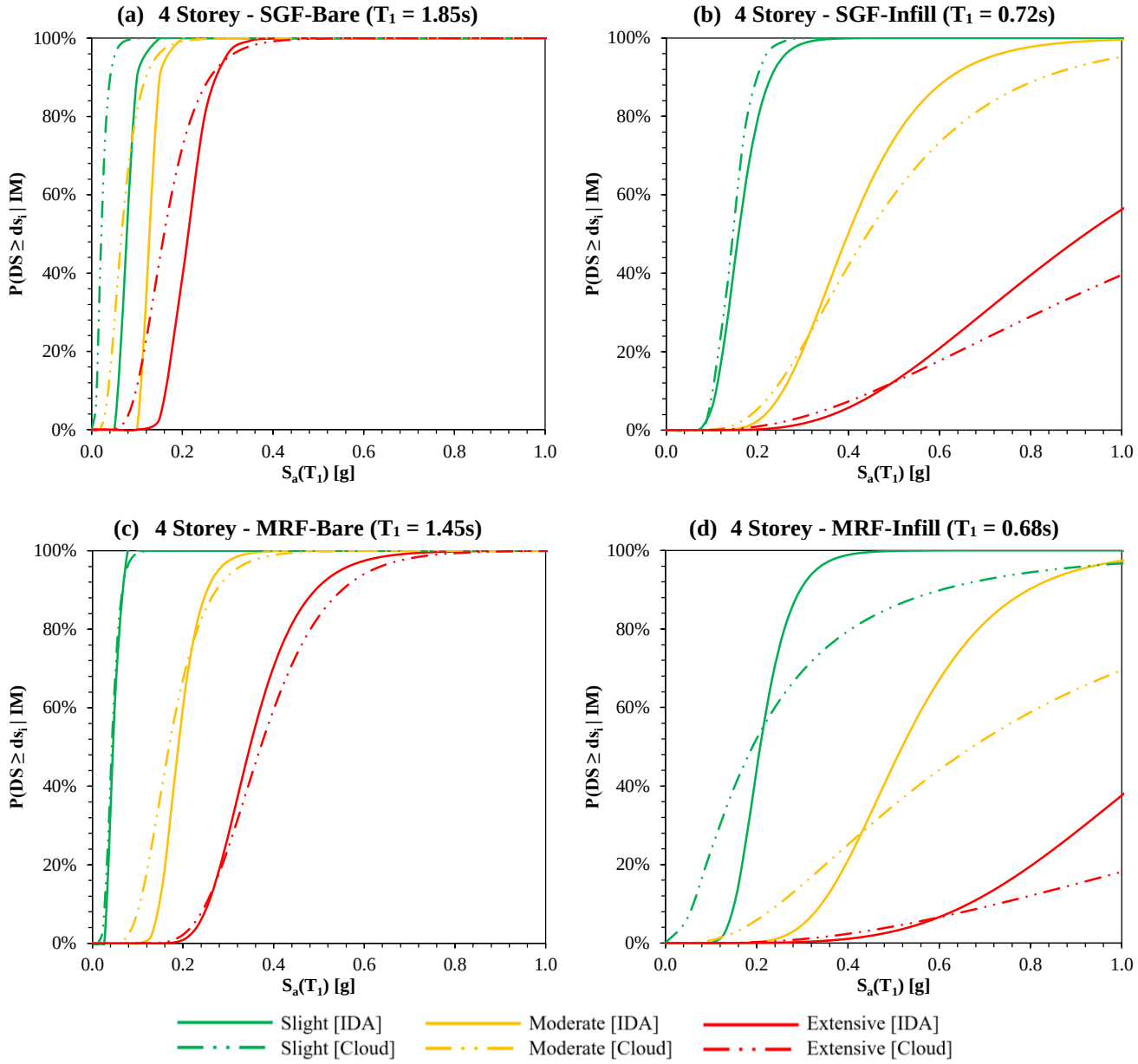

Fig. 12 - Fragility curves derived for 4 storey structures with different characteristics

Table 5 - IDA Fragility Functions - Median (μ [g]) and Dispersion (β) values for 4 storey structure

4 Storey IDA	SGF-Bare		SGR-Infill		MRF-Bare		MRF-Infill	
	μ	β	μ	β	μ	β	μ	β
Slight	0.05	0.71	0.16	0.29	0.05	0.08	0.21	0.27
Moderate	0.09	0.11	0.40	0.35	0.19	0.20	0.52	0.33
Extreme	0.16	0.25	0.92	0.53	0.35	0.27	1.12	0.40

Table 6 - Cloud Fragility Functions - Median (μ [g]) and Dispersion (β) values for 4 storey structure

4 Storey Cloud	SGF-Bare		SGR-Infill		MRF-Bare		MRF-Infill	
	μ	β	μ	β	μ	β	μ	β
Slight	0.02	0.51	0.14	0.24	0.04	0.34	0.19	0.90
Moderate	0.07	0.46	0.44	0.49	0.17	0.38	0.67	0.78
Extreme	0.16	0.38	1.23	0.77	0.37	0.31	2.17	0.85

7. Conclusion

The seismic behaviour of two (low-rise) and four (mid-rise) storey steel framed structures have been studied by means of different nonlinear dynamic methods (i.e. Cloud and IDA). Furthermore, the influence of masonry infill panels and also the quality of design codes have been examined by looking at the resultant IM-EDP and fragility curves. In order to characterise the intensity of the earthquakes, the spectral pseudo-acceleration corresponding to the first-mode elastic vibration period ($S_a(T_1)$) and 5% damping ratio is chosen. Maximum peak inter-story drift ratio (MIDR) has been adopted for seismic performance evaluation of the selected buildings.

For the cloud analysis 150 unscaled earthquake records of SIMBAD dataset have been applied, while for the IDA analysis 20 records were selected from FEMA P695 and each were scaled from 0.05g to 2.6g with steps of 0.05 (i.e. 1'040 performance points for each structural model). Due to nature of the SIMBAD earthquakes and depending on the capacity of the structures, most of the resultant performance points were concentrated at lower intensity measures. However, in case of IDA, as the applied intensity is under control, the structural performance associated to higher IM values can be recorded. Hence, in comparing the fragility curves of both methods, the similarly is more evident in lower damage limits (e.g. slight, and moderate) compared to extensive damage limit states. In comparison to Cloud analysis, a detailed IDA is computationally expensive, mainly due to higher numbers of NLTHA which need to be performed. Therefore, for lower intensities and depending on the required level of accuracy, one can select between Cloud or IDA.

8. References

[1] Nassirpour A, D'Ayala D (2014): Fragility Analysis of Mid-Rise Masonry Infilled Steel Frame (MISF) Structures. *Second European Conference on Earthquake Engineering and Seismology*, Istanbul, Turkey.
[2] Vamvatsikos D, Cornell CA (2002): Incremental Dynamic Analysis. *Earthquake Engineering & Structural Dynamics*, Volume 31, Issue 3, pp.491–514.
[3] Zareian F, Krawinkler H (2007): Assessment of Probability of Collapse and Design for Collapse Safety. *Earthquake Engineering & Structural Dynamics*, Volume 36, Issue 13, pp.1901–1914.
[4] Liao K, Wen Y, Foutch D (2007): Evaluation of 3D Steel Moment Frames under Earthquake Excitations. I: Modeling. *Journal of Structural Engineering*, Volume 133, Issue 3, pp.462-470.
[5] Tagawa H, MacRae G, Lowes L (2008): Probabilistic Evaluation of Seismic Performance of 3-Story 3D One- and Two-Way Steel Moment Frame Structures. *Earthquake Engineering & Structural Dynamics*, Volume 37, Issue 5, pp.681–696.
[6] Seismosoft (2013): SeismoStruct v7.0, A Computer Program for Static and Dynamic Nonlinear Analysis of Framed Structures.
[7] Crisafuli FJ, Carr AJ (2007): Proposed Macro-Model for the Analysis of Infilled Frame Structures. *Bulletin of the New Zealand Society for Earthquake Engineering*, Volume 40, No 2.
[8] Tasnimi A, Mohebkhah A (2011): Investigation on the Behaviour of Brick-Infilled Steel Frames with Openings, Experimental and Analytical Approaches. *Engineering Structures*, Volume 33, Issue 3, pp.968-980.
[9] Luco N, Bazzurro P (2007): Does Amplitude Scaling of Ground Motion Records Result in Biased Nonlinear Structural Drift Responses. *Earthquake Engineering & Structural Dynamics*, Volume 36, Issue 13, pp.1813–1835.
[10] Baker JW, Cornell AC (2006): Spectral Shape, Epsilon and Record Selection. *Earthquake Engineering & Structural Dynamics*, Volume 35, Issue 9, pp.1077–1095.
[11] Shome N, Cornell CA, Bazzurro P, Carballo JE (1998): Earthquakes, Records, and Nonlinear Responses. *Earthquake Spectra*, Volume 14, No. 3, pp.469-500.
[12] Iervolino I, Cornell CA (2005): Record Selection for Nonlinear Seismic Analysis of Structures. *Earthquake Spectra*, Volume 21, No. 3, pp.685-713.
[13] FEMA P695 (2009): Quantification of Building Seismic Performance Factors. *Federal Emergency Management Agency*, Washington D.C.
[14] Smerzini C, Galasso C, Iervolino I, Paoluccia R (2014): Ground Motion Record Selection Based on Broadband Spectral Compatibility. *Earthquake Spectra*, Volume 30, No. 4, pp.1427–1448.
[15] FEMA 354 (2000): A Policy Guide to Steel Moment-frame Construction. *Federal Emergency Management Agency*, Washington D.C.
[16] FEMA P-58 (2012): Seismic Performance Assessment of Buildings Volume 1 – Methodology. *Federal Emergency Management Agency*, Washington D.C.
[17] HAZUS - MH MR5 (2013): Advanced Engineering Building Module (AEBM) - Technical and User's Manual. *Federal Emergency Management Agency*, Washington D.C.
[18] FEMA 356 (2000): Pre-Standard and Commentary for The Seismic Rehabilitation of Buildings. *Federal Emergency Management Agency*, Washington D.C.
[19] Shinozuka M, Feng MQ, Kim HK, Kim SH (2000): Nonlinear Static Procedure for Fragility Curve Development. *ASCE Journal of Engineering Mechanics*, Volume 126, No.12, pp.1267–1295.
[20] Baker JW (2015): Efficient Analytical Fragility Function Fitting Using Dynamic Structural Analysis. *Earthquake Spectra*, Volume 31, Issue 1, pp.579-599.
[21] Basöz N, Kiremidjian AS (1998): Evaluation of Bridge Damage Data from the Loma Prieta and Northridge, CA Earthquakes. Technical Report MCEER-98-0004, *Multidisciplinary Centre for Earthquake Engineering Research*, Buffalo, New York.
[22] Lallemant D, Kiremidjian A, Burton H (2015): Statistical Procedures for Developing Earthquake Damage Fragility Curves. *Earthquake Engineering & Structural Dynamics*, Volume 44, Issue 9, pp.1373–1389.